

## **Keggin-type polyoxotungstates in the Hofmeister Classification**

Sa Yao,<sup>a</sup> Clément Falaise,<sup>a</sup> Anton A. Ivanov,<sup>a,b</sup> Nathalie Leclerc,<sup>a</sup> Max Hohenschutz,<sup>d</sup> Mohamed Haouas,<sup>\*a</sup> David Landy,<sup>c</sup> Michael Shestopalov,<sup>b</sup> Pierre Bauduin,<sup>d</sup> and Emmanuel Cadot<sup>\*a</sup>

### ***Electronic Supplementary Information***

## Table of contents:

### Part 1: Single crystal X-ray diffraction

- 1- Selected crystallographic parameters
- 2- Structural views of  $\text{PW}_{12}@CD$
- 3- Structural views of  $\text{BW}_{12}\cdot 2CD$

### Part 2: Isothermal titration calorimetry (ITC)

- 1-  $\gamma$ -CD/ $\text{BW}_{12}$  system
- 2-  $\gamma$ -CD/ $\text{SiW}_{12}$  system
- 3-  $\gamma$ -CD/ $\text{PW}_{12}$  system

### Part 3: Electrochemistry

- 1-  $\gamma$ -CD/ $\text{BW}_{12}$  system
- 2-  $\gamma$ -CD/ $\text{SiW}_{12}$  system
- 3-  $\gamma$ -CD/ $\text{PW}_{12}$  system

### Part 4: NMR studies in solution

- 1-  $^1\text{H}$  NMR spectra of  $\gamma$ -CD/ $\text{XW}_{12}$  systems in  $\text{D}_2\text{O}$  at fixed  $[\text{CD}] = 2 \text{ mM}$
- 2- Determining affinity constant from  $^1\text{H}$  chemical shifts
- 3- Modeling  $^1\text{H}$  DOSY data

### Part 5: SAXS measurements

- 1- Experimental
- 2- SAXS spectra of Keggin POMs in water
- 3- SAXS spectra of Keggin POMs in presence of  $\text{C}_8\text{E}_4$

### Part 6: Characterizations by FT-IR spectroscopy

- 1- FT-IR spectrum of compound  $\text{PW}_{12}@CD$
- 2- FT-IR spectrum of compound  $\text{BW}_{12}\cdot 2CD$

## Part 1: Single crystal X-ray diffraction

### 1- Selected crystallographic parameters

**Table S1: Selected crystallographic parameters of the single-crystal X-ray diffraction structural analysis**

Identification code	PW <sub>12</sub> @CD	BW <sub>12</sub> •2CD
CCDC number	2015681	2015682
Empirical formula	C <sub>48</sub> H <sub>54</sub> Na <sub>0.67</sub> O <sub>87</sub> PW <sub>12</sub>	C <sub>96</sub> H <sub>108</sub> BCsO <sub>120</sub> W <sub>12</sub>
Formula weight	4275.39	5531.74
Temperature/K	210	210
Crystal system	cubic	Tetragonal
Space group	I23	P4 <sub>2</sub> ,2
a/Å	41.7867(14)	23.199(2)
b/Å	41.7867(14)	23.199(2)
c/Å	41.7867(14)	17.304(2)
α/°	90	90
β/°	90	90
γ/°	90	90
Volume/Å <sup>3</sup>	72965(7)	9313(2)
Z	24	2
ρ <sub>calc</sub> /g/cm <sup>3</sup>	2.335	1.973
μ/mm <sup>-1</sup>	11.417	7.672
F(000)	46760	5184
Crystal size/mm <sup>3</sup>	0.15 × 0.14 × 0.12	0.15 × 0.15 × 0.1
Radiation	MoKα (λ = 0.71073)	MoKα (λ = 0.71073)
2θ range for data collection/°	3.082 to 54.37	4.578 to 50.288
Index ranges	-53 ≤ h ≤ 53 -38 ≤ k ≤ 53 -53 ≤ l ≤ 53	-27 ≤ h ≤ 27 -27 ≤ k ≤ 27 -20 ≤ l ≤ 20
Reflections collected	670750	238197
Independent reflections	25540 R <sub>int</sub> = 0.0853 R <sub>sigma</sub> = 0.0457	8331 R <sub>int</sub> = 0.0979 R <sub>sigma</sub> = 0.0251
Data/restraints/parameters	25540/36/1009	8331/53/530
Goodness-of-fit on F <sup>2</sup>	1.027	1.109
Final R indexes [I ≥ 2σ (I)]	R <sub>1</sub> = 0.0328 wR <sub>2</sub> = 0.0806	R <sub>1</sub> = 0.0441 wR <sub>2</sub> = 0.1159
Final R indexes [all data]	R <sub>1</sub> = 0.0417 wR <sub>2</sub> = 0.0825	R <sub>1</sub> = 0.0481 wR <sub>2</sub> = 0.1191
Largest diff. peak/hole / e Å <sup>-3</sup>	2.30/-1.53	1.81/-1.90

## 2- Structural views of $\text{PW}_{12}\text{@CD}$

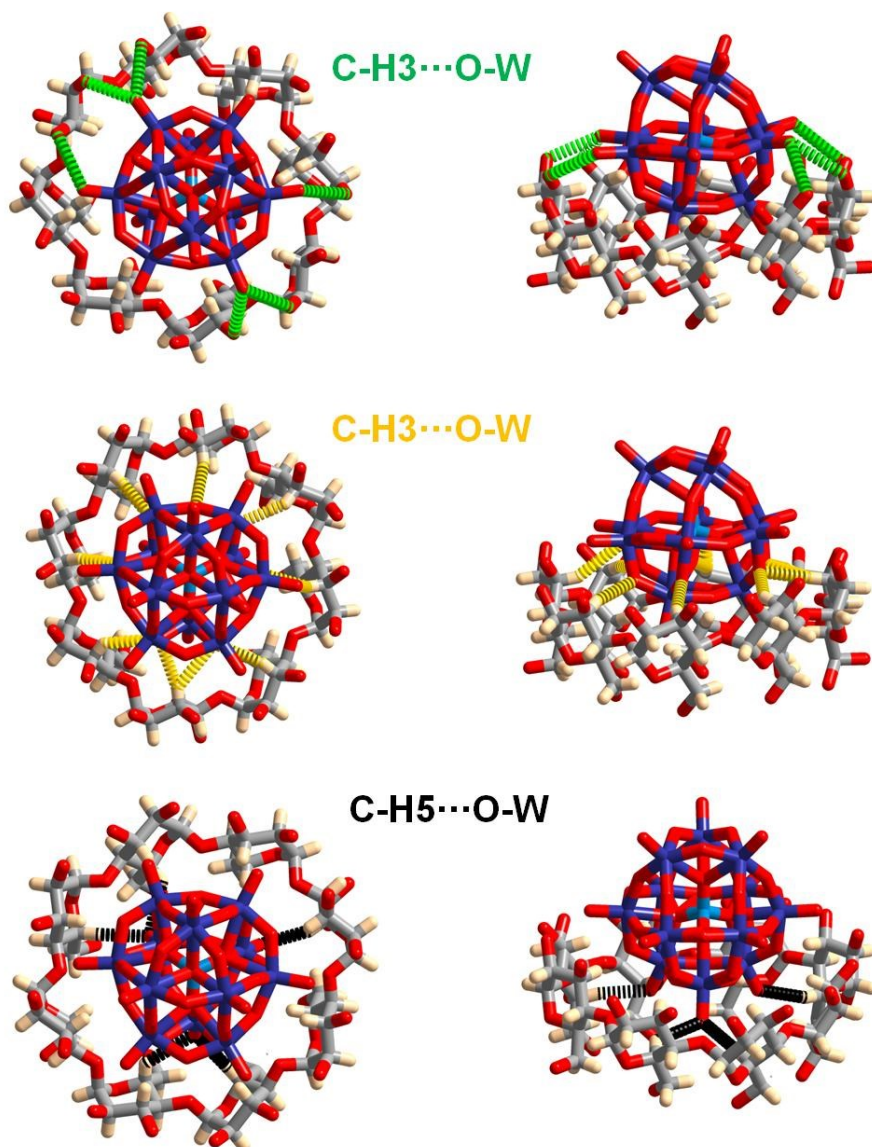


**Figure S1:** Illustration of the different supramolecular interactions involved in the 1:1 host-guest complex  $\{\text{PW}_{12}\text{O}_{40}\text{@CD}\}^{3-}$  in  $\text{PW}_{12}\text{@CD}$ . The terminal and bridging oxygen atoms of the  $\text{PW}_{12}\text{O}_{40}^{3-}$  entity interact with CD through numerous H-bonds (green), and many short contacts with H3 (yellow) and H5 (black).

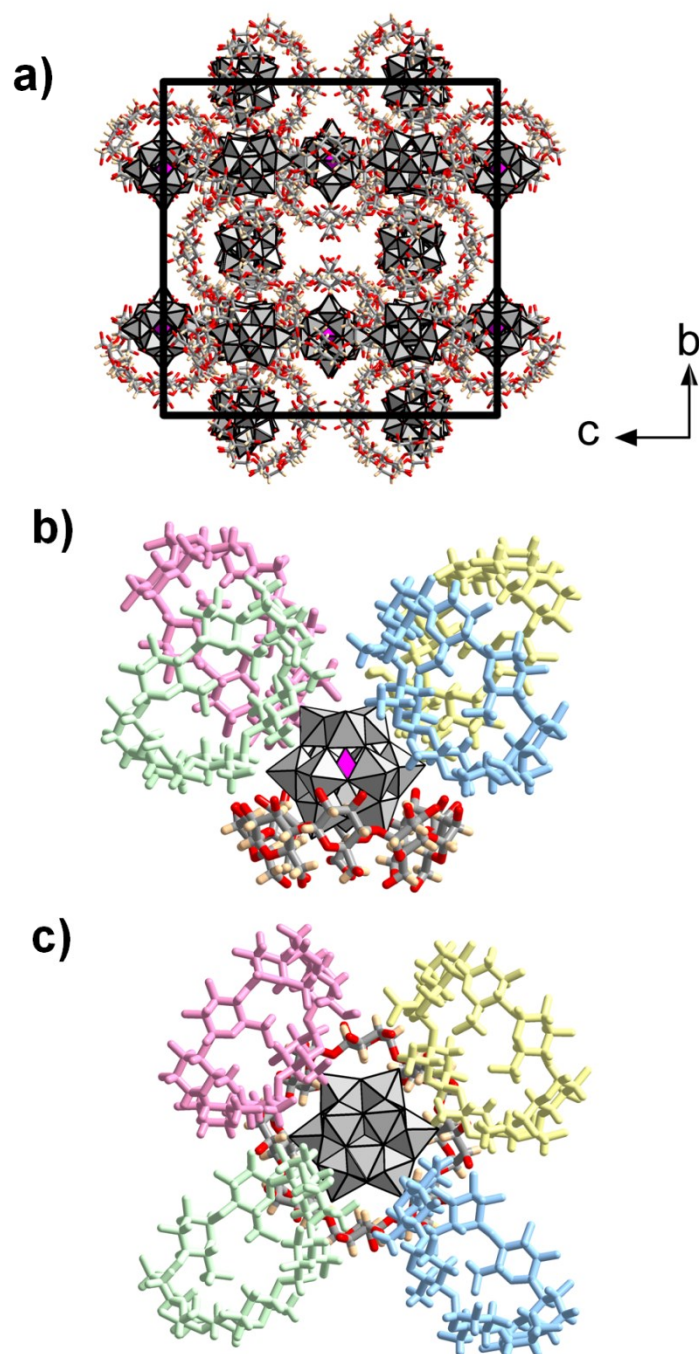


**Figure S2:** a) View of the cubic unit cell of the compound  $\text{PW}_{12}\text{@CD}$ . Free water molecules and sodium cations are omitted for clarity. b and c) Illustration of the structural arrangement between the 1:1 host-guest complex  $\{\text{PW}_{12}\text{O}_{40}\text{@CD}\}^{3-}$  and the four CDs of other inclusion complexes. The supramolecular interaction (short contacts) are observed between the uncomplexed part of the POM unit and the external surface of four CDs. For clarity, each CD interacting through its external surface is shown with different colors.

### 3- Structural views of $\text{BW}_{12}\cdot 2\text{CD}$

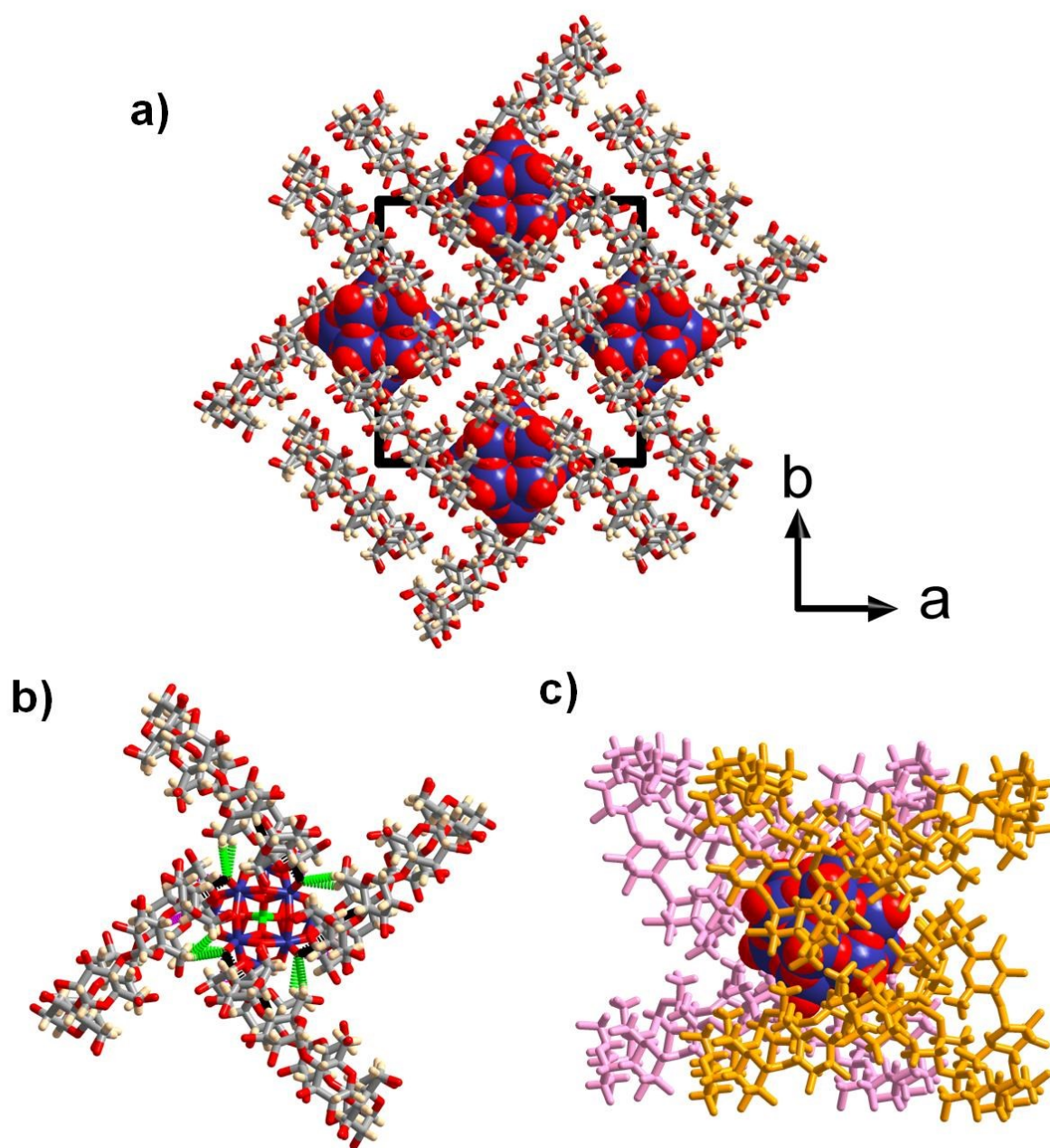


**Figure S3:** a) View of the tetragonal unit cell of the compound  $\text{BW}_{12}\cdot 2\text{CD}$  along  $c$  axis. Free water molecules and counter cations are omitted for clarity. b) and c) Illustrations of the CD around  $\{\text{BW}_{12}\text{O}_{40}\}^{5-}$ . Each POM unit interacts with eight CD hosts through their external surface (H1, H2 H4 and H6).

## Part 2: Isothermal titration calorimetry (ITC)

1-  $\gamma$ -CD/ $\text{BW}_{12}$  system

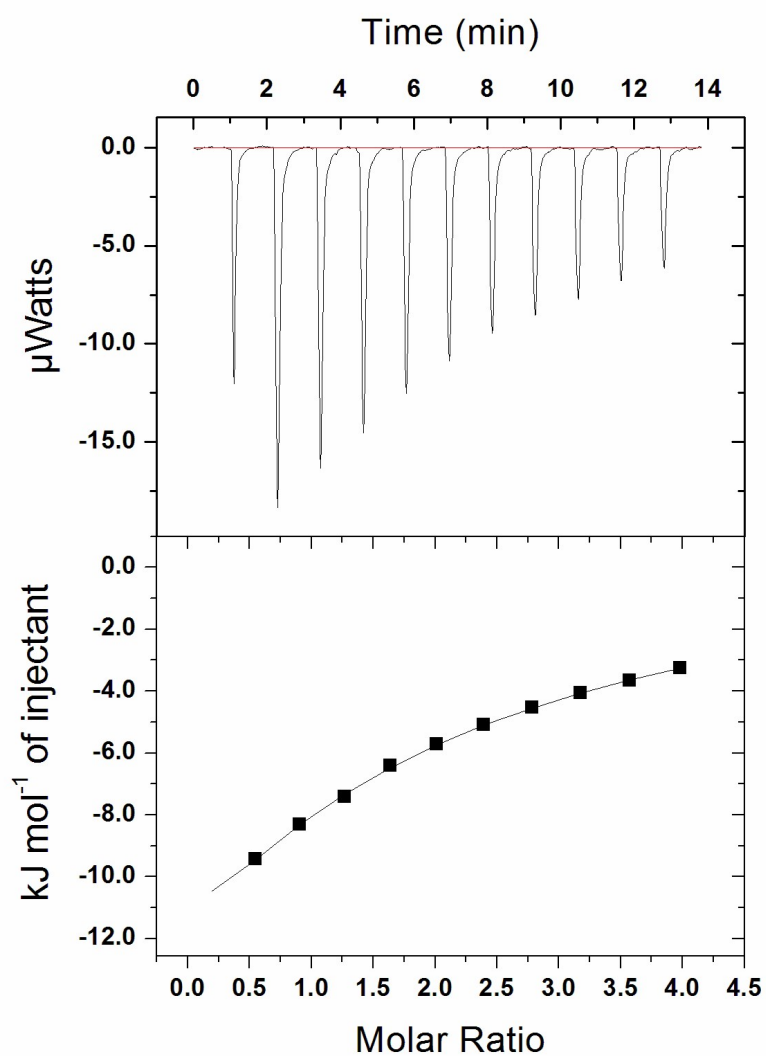


**Figure S4.** ITC thermogram (upper part) and isotherm (lower part) for the system  $\gamma$ -CD/ $[\text{BW}_{12}\text{O}_{40}]^{5-}$  at 298K. Dots and lines correspond to experimental and theoretical heats, respectively.



2-  $\gamma$ -CD/SiW<sub>12</sub> system

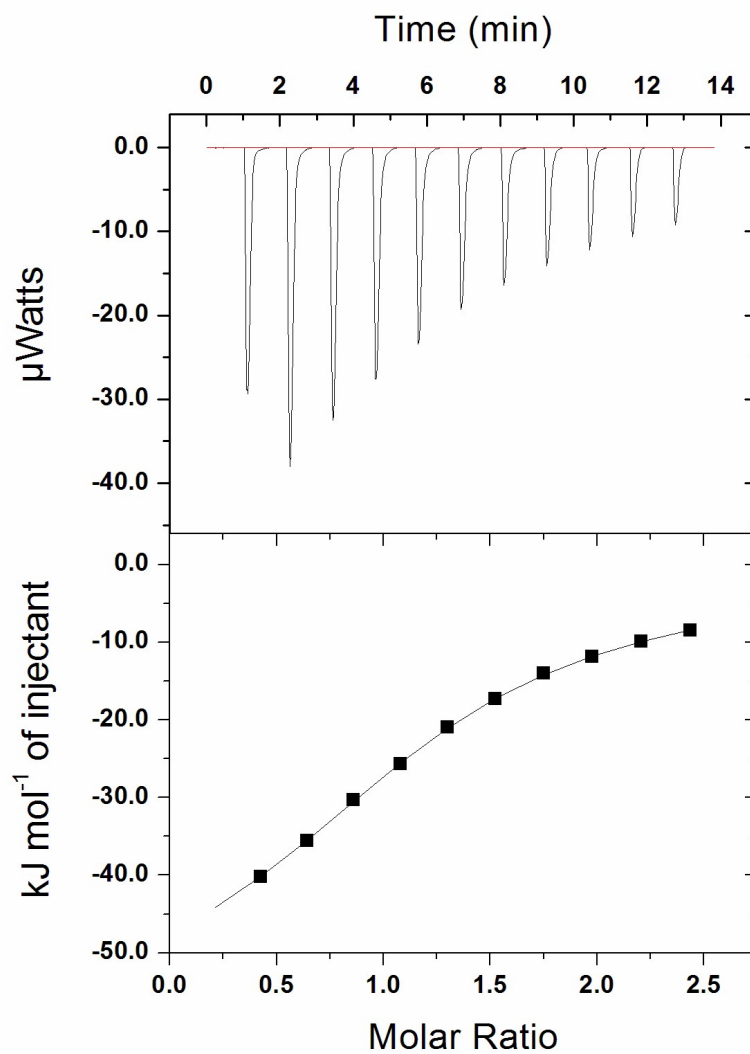


**Figure S5.** ITC thermogram (upper part) and isotherm (lower part) for the system  $\gamma$ -CD/[SiW<sub>12</sub>O<sub>40</sub>]<sup>4-</sup> at 298K. Dots and lines correspond to experimental and theoretical heats, respectively.



3-  $\gamma$ -CD/ $\text{PW}_{12}$  system

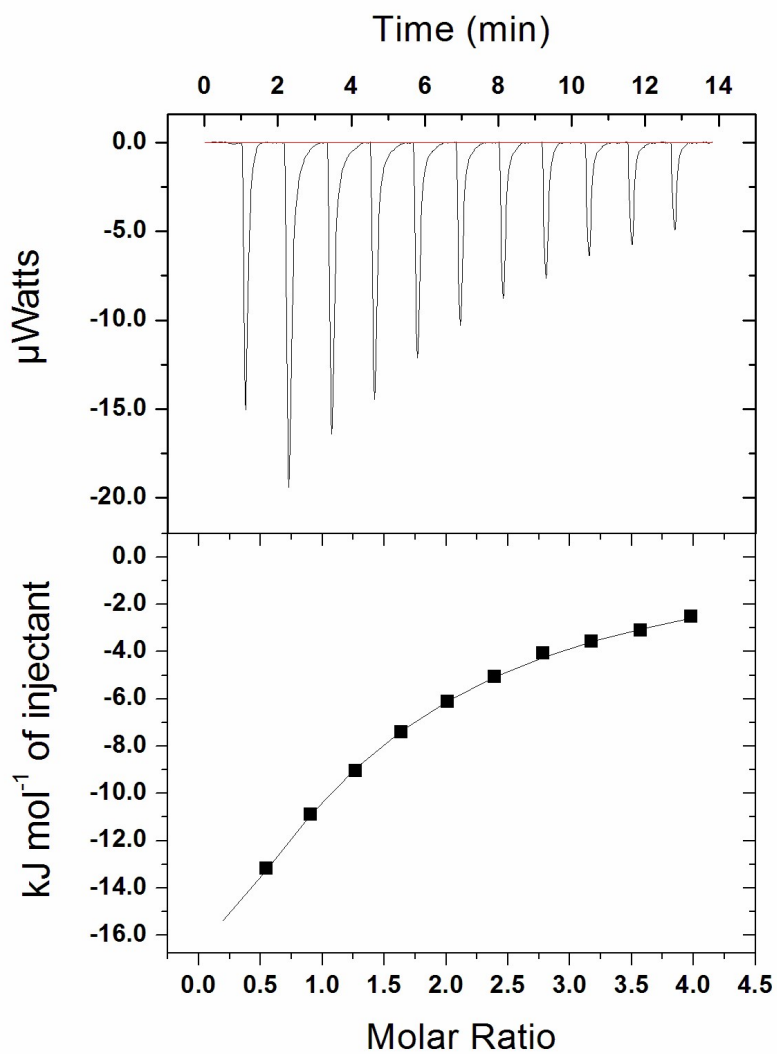


**Figure S6.** ITC thermogram (upper part) and isotherm (lower part) for the system  $\gamma$ -CD/ $[\text{PW}_{12}\text{O}_{40}]^{3-}$  at 298K. Dots and lines correspond to experimental and theoretical heats, respectively.

### Part 3: Electrochemistry

Assuming complexation processes and electron transfers are fast and reversible, the observed potentials for the 1<sup>st</sup> and 2<sup>nd</sup> wave can be described by the following equations:

$$E_{peak,1} = E_1^0 + \frac{RT}{F} \ln \frac{(1 + K_{1:1}^{ox} [CD]_{eq} + K_{1:1}^{ox} K_{1:2}^{ox} [CD]_{eq}^2)}{(1 + K_{1:1}^{red1} [CD]_{eq} + K_{1:1}^{red1} K_{1:2}^{red1} [CD]_{eq}^2)} \quad (1)$$

$$E_{peak,2} = E_2^0 + \frac{RT}{F} \ln \frac{(1 + K_{1:1}^{red1} [CD]_{eq} + K_{1:1}^{red1} K_{1:2}^{red1} [CD]_{eq}^2)}{(1 + K_{1:1}^{red2} [CD]_{eq} + K_{1:1}^{red2} K_{1:2}^{red2} [CD]_{eq}^2)} \quad (2)$$

#### 1- $\gamma$ -CD/BW<sub>12</sub> system

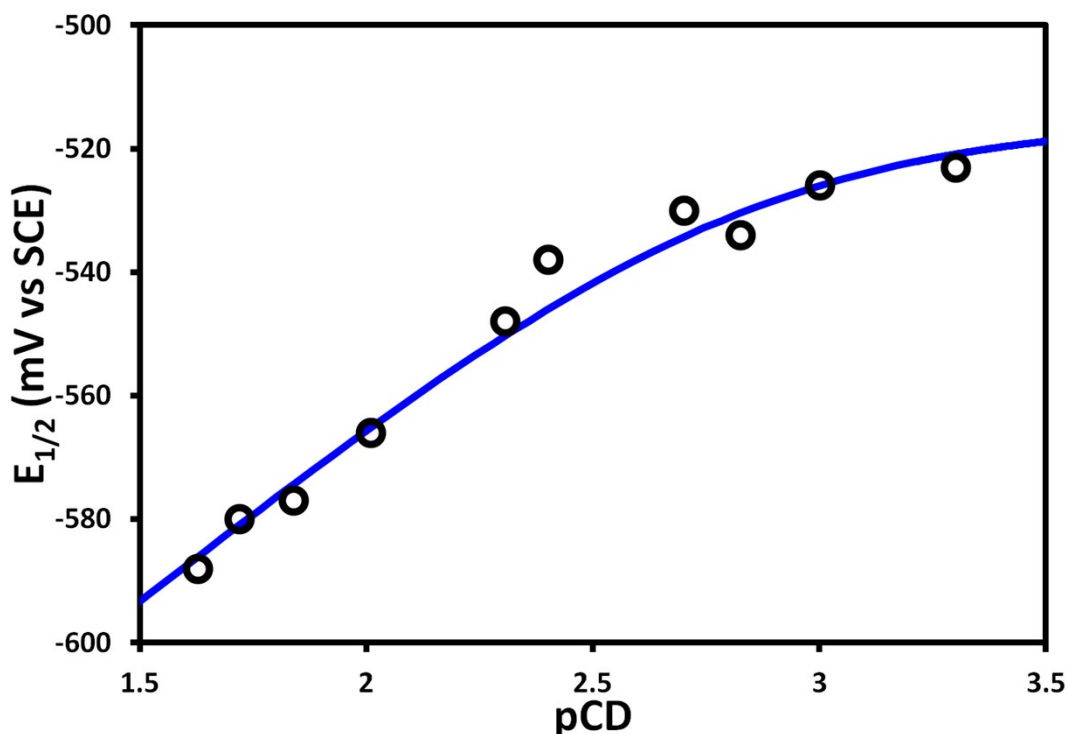


**Figure S7.** Variation of potential of the first wave observed in CV of 0.5 mM [BW<sub>12</sub>O<sub>40</sub>]<sup>5-</sup> as a function of pCD (pCD = -log[CD]). The curve corresponds to the best fit of experimental measurements (open circles), calculated with equation (1).

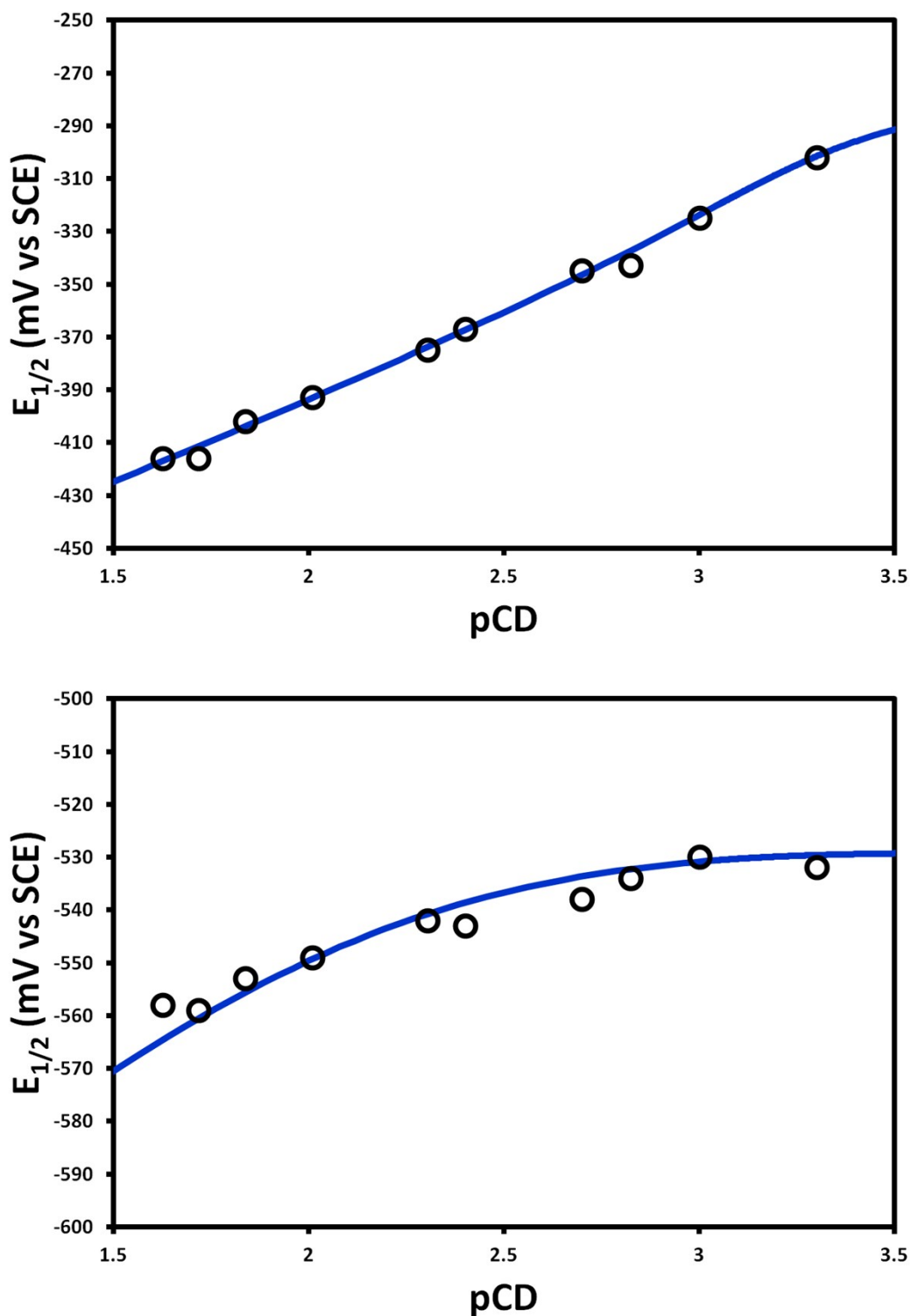


**Figure S8.** Variation of potential of the (top) first and (down) second wave observed in CV of 0.5 mM [SiW<sub>12</sub>O<sub>40</sub>]<sup>4-</sup> as a function of pCD (pCD = -log[CD]). The curves correspond to the best fits of experimental measurements (open circles), calculated with equations (1) and (2) for the first and second waves respectively.

32  $\gamma$ -CD/PW<sub>12</sub> system

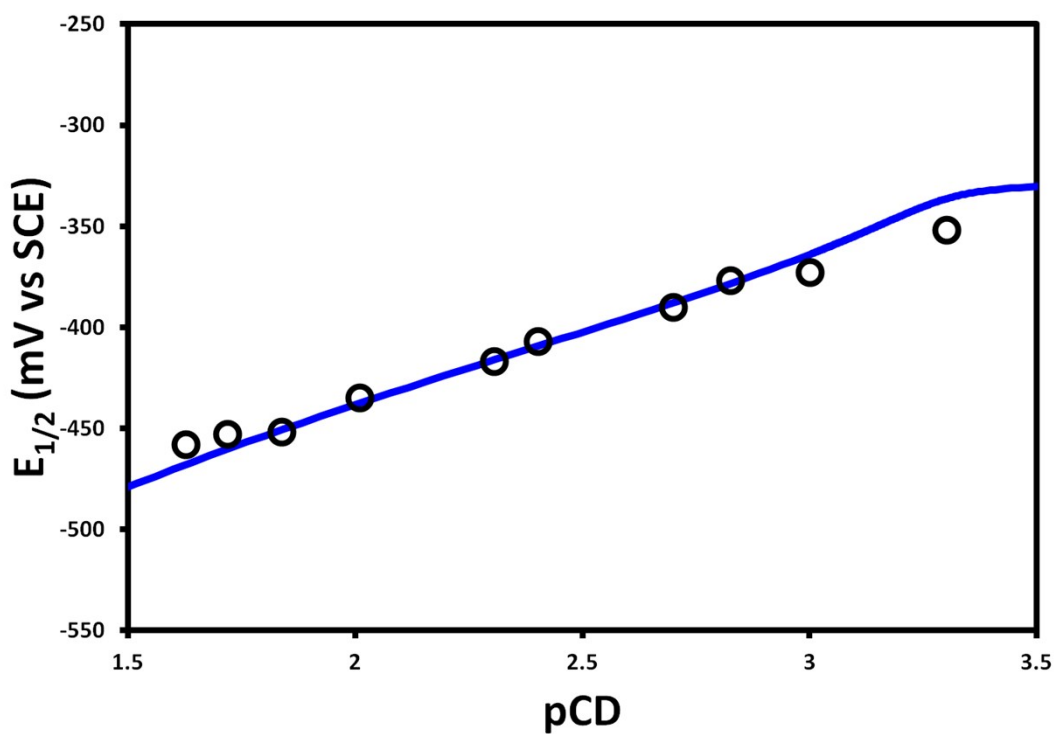
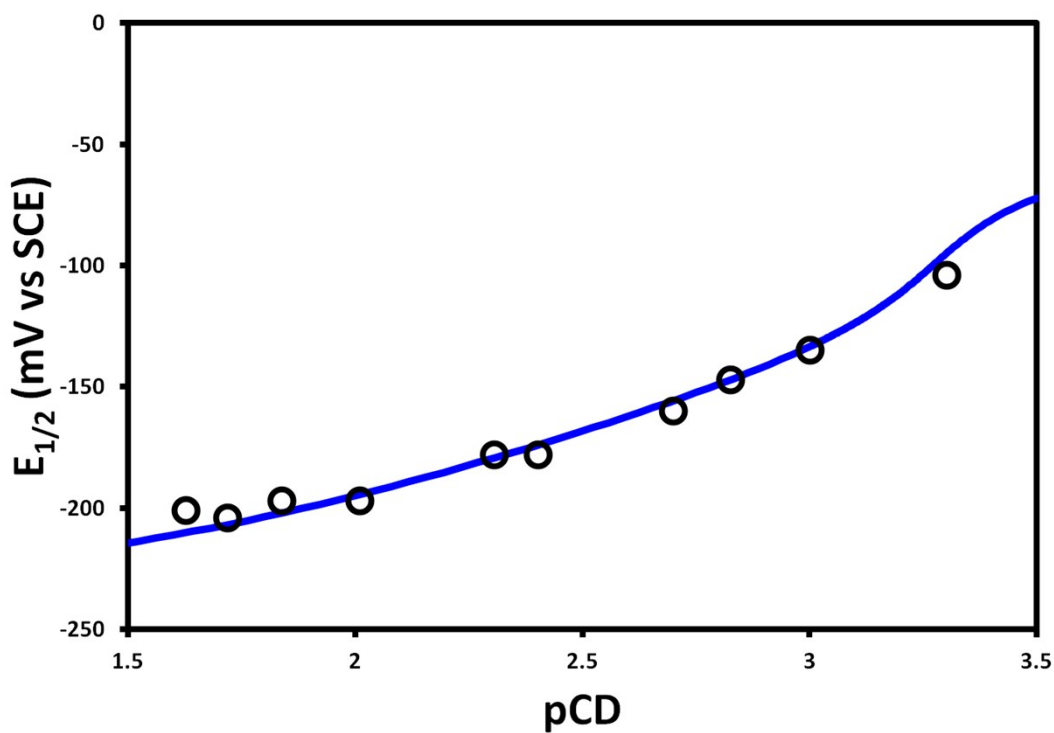


**Figure S9.** Variation of potential of the (top) first and (down) second wave observed in CV of 0.5 mM [PW<sub>12</sub>O<sub>40</sub>]<sup>3-</sup> as a function of pCD (pCD = -log[CD]). The curves correspond to the best fits of experimental measurements (open circles), calculated with equations (1) and (2) for the first and second waves respectively.

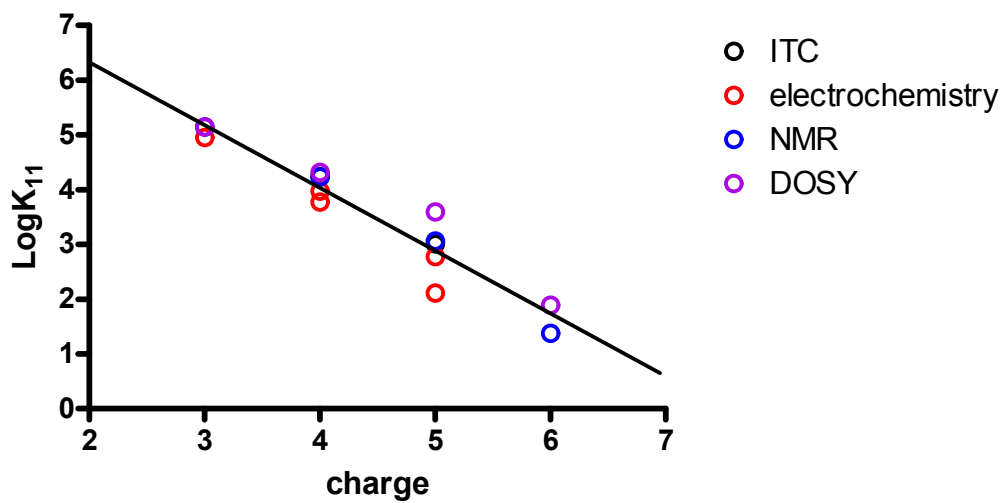


**Figure S10.** Variation of binding constants in 1:1 adduct between  $[XW_{12}O_{40}]^{n-}$  POM and  $\gamma$ -CD as a function of ionic charge  $n$  of the Keggin-type anion as measured by ITC, electrochemistry and NMR ( $^1\text{H}$  chemical shift and DOSY).

## Part 4: NMR studies in solution

1-  $^1\text{H}$  NMR spectra of  $\gamma\text{-CD}/\text{XW}_{12}$  systems in  $\text{D}_2\text{O}$  at fixed  $[\text{CD}] = 2 \text{ mM}$

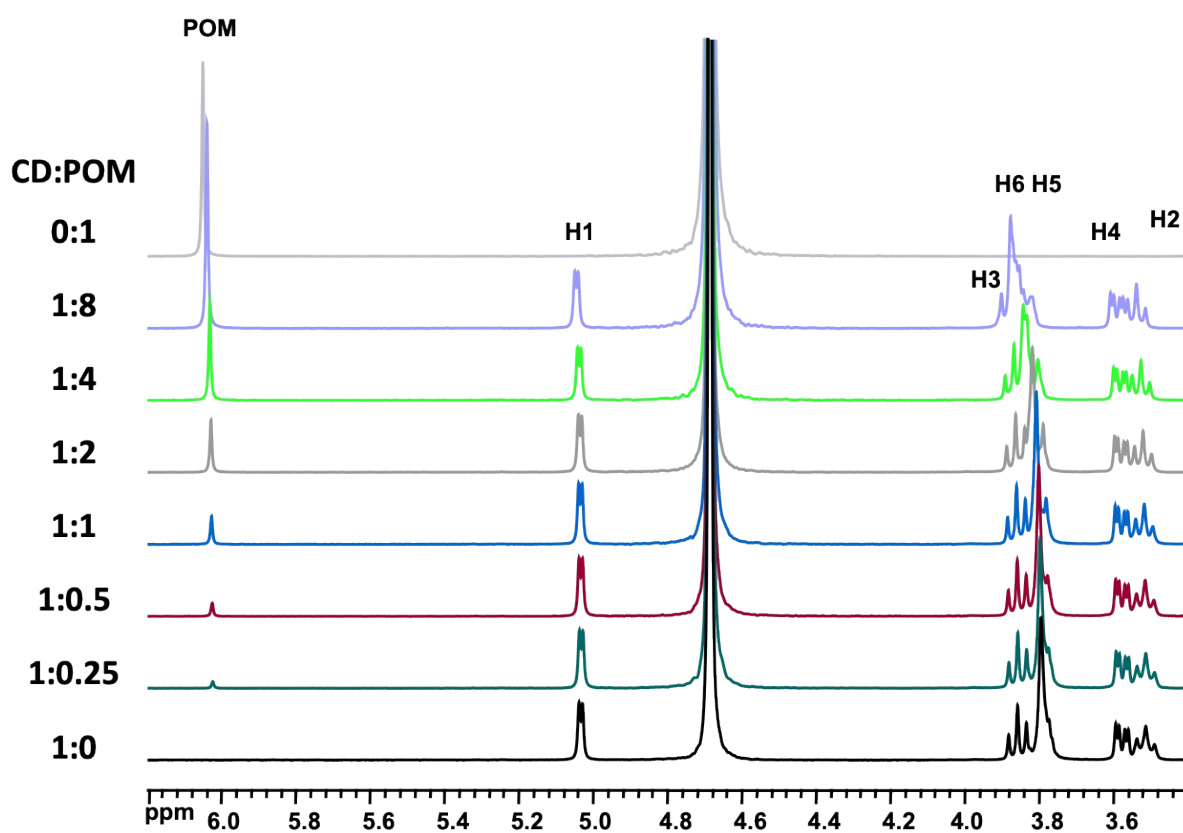


**Figure S11.**  $^1\text{H}$  NMR spectra resulting from the titration of  $2 \text{ mmol}\cdot\text{L}^{-1}$  aqueous solution of  $\gamma\text{-CD}$  by  $[\text{H}_2\text{W}_{12}\text{O}_{40}]^{6-}$  POM.

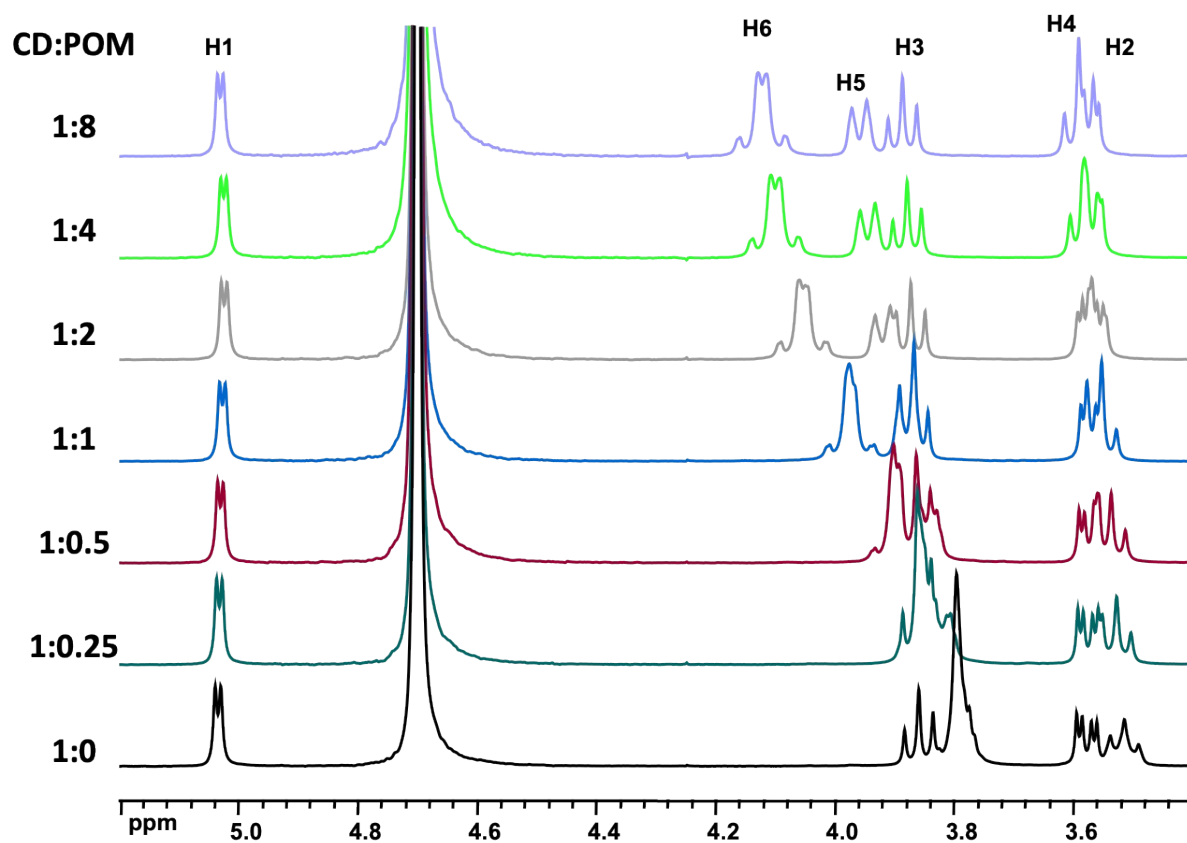


**Figure S12.** <sup>1</sup>H NMR spectra resulting from the titration of 2 mmol.L<sup>-1</sup> aqueous solution of  $\gamma$ -CD by [BW<sub>12</sub>O<sub>40</sub>]<sup>5-</sup> POM.



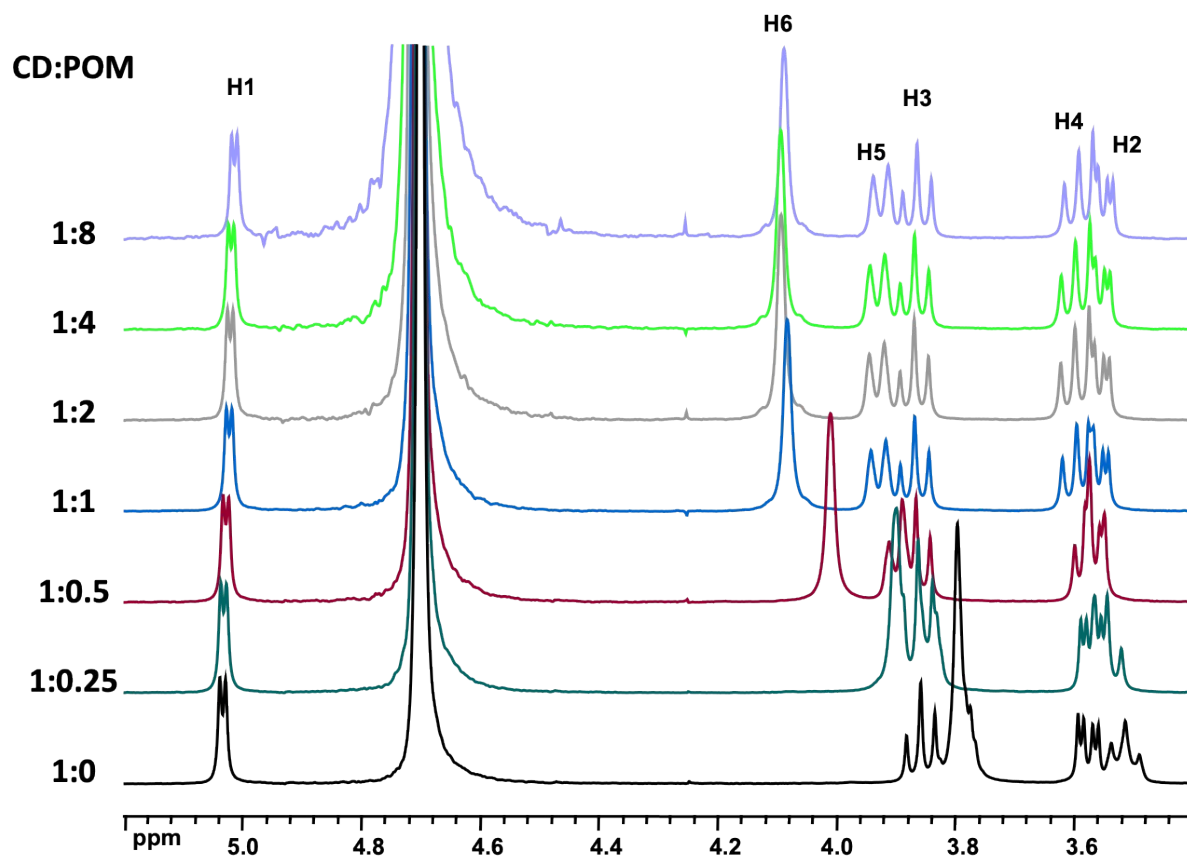


**Figure S13.**  $^1\text{H}$  NMR spectra resulting from the titration of  $2 \text{ mmol}\cdot\text{L}^{-1}$  aqueous solution of  $\gamma$ -CD by  $[\text{SiW}_{12}\text{O}_{40}]^{4-}$  POM.

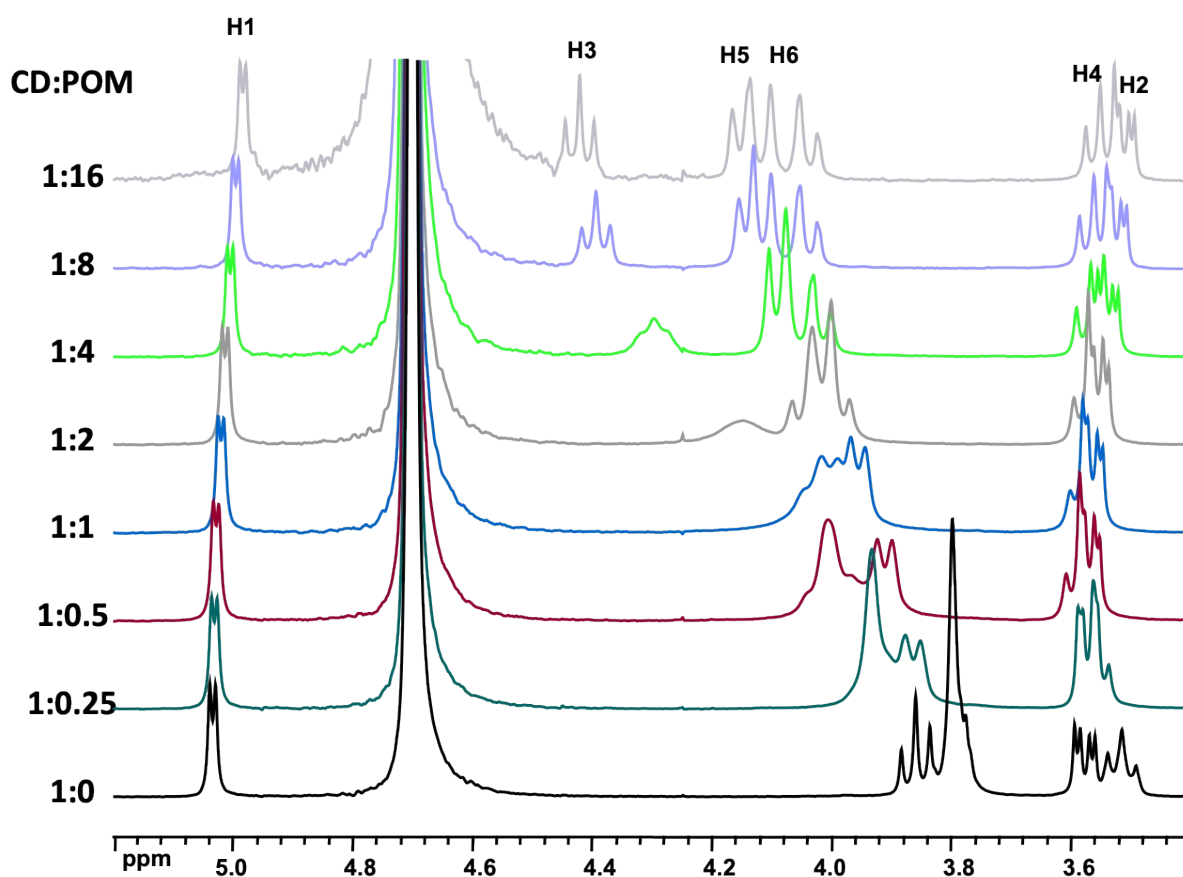


**Figure S14.**  $^1\text{H}$  NMR spectra resulting from the titration of  $2 \text{ mmol.L}^{-1}$  aqueous solution of  $\gamma$ -CD by  $[\text{PW}_{12}\text{O}_{40}]^{3-}$  POM.

## 2- Determining affinity constant from $^1\text{H}$ chemical shifts

In conditions of fast exchange regime with respect to the NMR time scale, the observed chemical shift of CD corresponds to a weighted average of the chemical shift of the individual species, i.e., the free CD ( $\delta_1$ ), the 1:1 POM:CD complex ( $\delta_2$ ), and the 1:2 POM:CD complex ( $\delta_3$ ):

$$\delta_{\text{obs}} = X_1\delta_1 + X_2\delta_2 + X_3\delta_3 \quad (3)$$

In the simplest case of single step complexation, the 1:2 species is negligible and the observed chemical shifts can be written:

$$\delta_{\text{obs}} = X_1\delta_1 + X_2\delta_2 = X_1\delta_1 + (1-X_1)\delta_2 \quad (4)$$

As the molar fraction  $X_1$  is a function of equilibrium constant  $K$  and initial CD concentration  $C_{\text{CD}}$ , eq. 2 can be expressed as a function of molar ration  $R = \text{POM}/\text{CD}$ :

$$\delta_{\text{obs}} = \delta_1 \frac{(KC_{\text{CD}} - KC_{\text{CD}}R - 1) + \sqrt{(KC_{\text{CD}}R - KC_{\text{CD}} + 1)^2 + 4KC_{\text{CD}}}}{2KC_{\text{CD}}} + \delta_2 \left( \frac{(KC_{\text{CD}} + KC_{\text{CD}}R + 1) - \sqrt{(KC_{\text{CD}}R - KC_{\text{CD}} + 1)^2 + 4KC_{\text{CD}}}}{2KC_{\text{CD}}} \right) \quad (5)$$

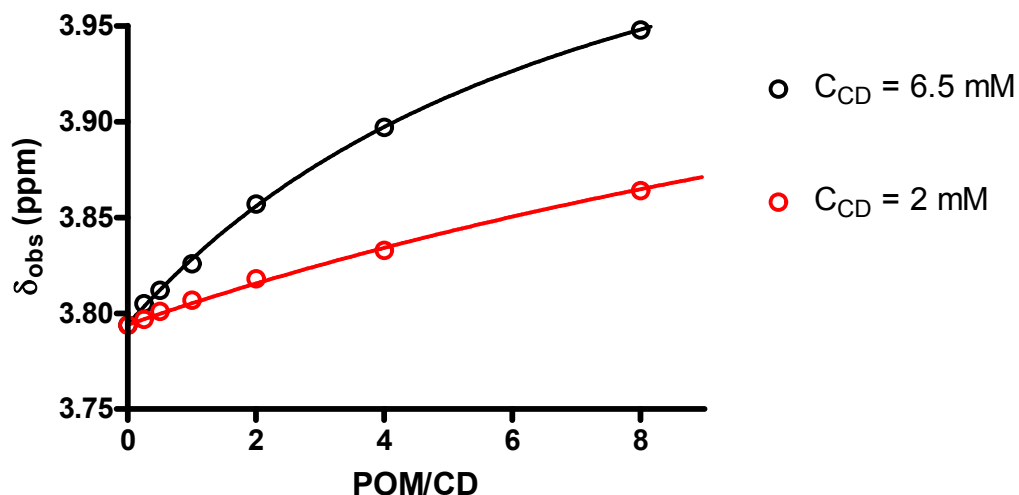


**Figure S15.** Modeling of observed  $^1\text{H}$  NMR chemical shifts of most affected  $\gamma$ -CD proton (H6) as a function of POM/CD molar ratio during titration of  $\gamma$ -CD by  $[\text{H}_2\text{W}_{12}\text{O}_{40}]^{6-}$  for two different CD concentration (2 and 6.5 mM). The lines represent calculated curves using equation (5) with optimized  $K = 23 \pm 1 \text{ M}^{-1}$  and chemical shifts  $\delta_2 = 4.09 \pm 0.01$  ppm.

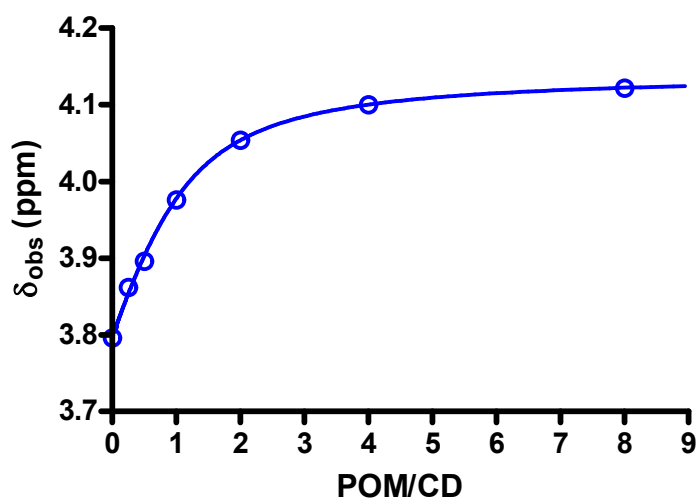


**Figure S16.** Modeling of observed  $^1\text{H}$  NMR chemical shifts of most affected  $\gamma$ -CD proton (H6) as a function of POM/CD molar ratio during titration of 2 mM  $\gamma$ -CD by  $[\text{BW}_{12}\text{O}_{40}]^{5-}$ . The line represents calculated curve using equation (5) with optimized  $K = 1100 \pm 100 \text{ M}^{-1}$  and chemical shifts  $\delta_2 = 4.143 \pm 0.006$  ppm.

### 3- Modeling <sup>1</sup>H DOSY data

Like chemical shift, the observed diffusion coefficient  $D_{\text{obs}}$  of a species exchanging its position between free and different binding states could be written as a weighted average of diffusion constants of each situation when the process is fast compared to the NMR time scale. In our case of CD in presence of Keggin POM, the CD could be present as free species (#1) and depending on the nature of the POM as either 1:1 POM: CD complex (#2) or 1:1 and 1:2 POM:CD (#3) complexes.

Case I : one-step complexation

$$D_{\text{obs}} = X_1 D_1 + X_2 D_2 \quad (6)$$

$$D_{\text{obs}} = D_1 \frac{(KC_{\text{CD}} - KC_{\text{CD}}R - 1) + \sqrt{(KC_{\text{CD}}R - KC_{\text{CD}} + 1)^2 + 4KC_{\text{CD}}}}{2KC_{\text{CD}}} + D_2 \frac{(KC_{\text{CD}} + KC_{\text{CD}}R + 1) - \sqrt{(KC_{\text{CD}}R - KC_{\text{CD}} + 1)^2 + 4KC_{\text{CD}}}}{2KC_{\text{CD}}} \quad (7)$$

Case II : two-step complexation

$$D_{\text{obs}} = X_1 D_1 + X_2 D_2 + X_3 D_3 \quad (8)$$

The fraction of free CD  $X_1$  can be obtained from the following relation:

$$abX_1^3 + (2abR - ab + a)X_1^2 + (aR - a + 1)X_1 = 1 \quad (9)$$

$$\text{with } a = K_{11}C_{\text{CD}} \text{ and } b = K_{12}C_{\text{CD}}$$

where  $K_{11}$  and  $K_{12}$  are equilibrium constants for step 1 and step 2 processes

The fractions of 1:1 and 1:2 POM:CD complexes, respectively  $X_2$  and  $X_3$  are calculated as follows:

$$X_2 = \frac{1 - X_1}{1 + 2bX_1} \quad (10) \quad X_3 = 1 - X_1 - X_2 \quad (11)$$

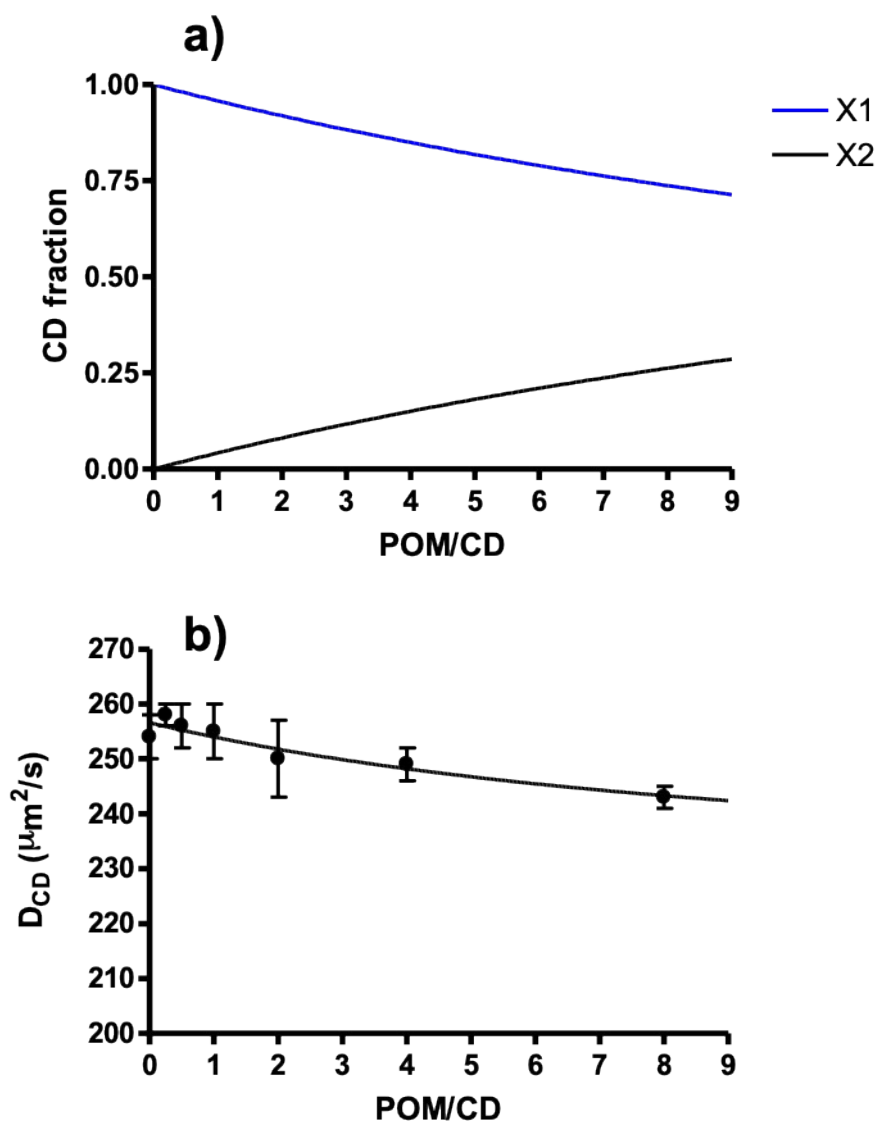


**Figure S17.** (a)  $\gamma$ -CD species distribution in one-step process model ( $X_1$ : free CD and  $X_2$ : 1:1 POM-CD complex) as a function of POM/CD molar ratio  $R$  in the NMR experimental conditions for titration of 2 mM  $\gamma$ -CD by  $[\text{H}_2\text{W}_{12}\text{O}_{40}]^{6-}$ . (b) Modeling of observed diffusion coefficient of  $\gamma$ -CD as a function of POM/CD molar ratio during titration of 2 mM  $\gamma$ -CD by  $[\text{H}_2\text{W}_{12}\text{O}_{40}]^{6-}$ . The lines represent calculated curves using equations 6 and 7 with optimized  $K = 50 \pm 10 \text{ M}^{-1}$  and diffusion coefficients limits for free CD and 1:1 complex:  $D_1 = 254 \mu\text{m}^2/\text{s}$  and  $D_2 = 226 \mu\text{m}^2/\text{s}$ .

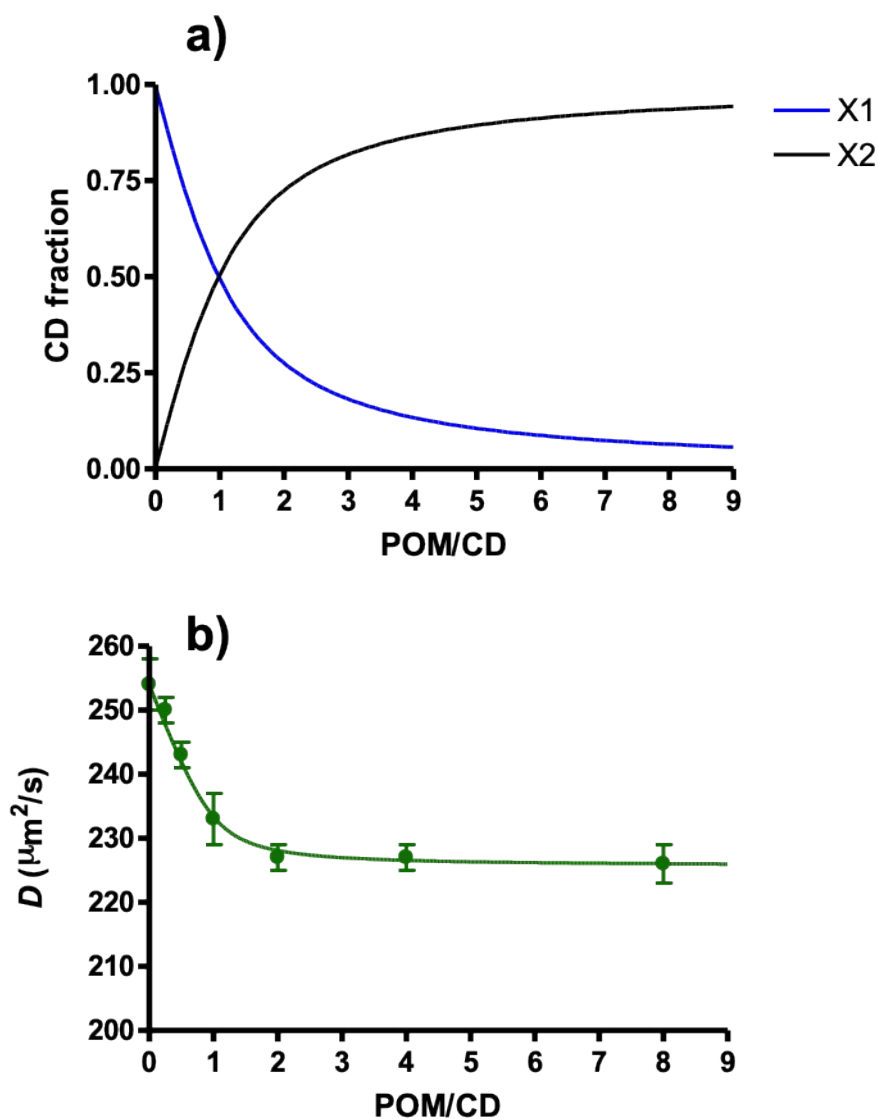


**Figure S18.** (a)  $\gamma$ -CD species distribution in one-step process model ( $X_1$ : free CD and  $X_2$ : 1:1 POM-CD complex) as a function of POM/CD molar ratio  $R$  in the NMR experimental conditions for titration of 2 mM  $\gamma$ -CD by  $[\text{BW}_{12}\text{O}_{40}]^{5-}$ . (b) Modeling of observed diffusion coefficient of  $\gamma$ -CD as a function of POM/CD molar ratio during titration of 2 mM  $\gamma$ -CD by  $[\text{BW}_{12}\text{O}_{40}]^{5-}$ . The lines represent calculated curves using equations 6 and 7 with optimized  $K = 3000 \text{ M}^{-1}$  and diffusion coefficients limits for free CD and 1:1 complex:  $D_1 = 254 \mu\text{m}^2/\text{s}$  and  $D_2 = 226 \mu\text{m}^2/\text{s}$ .

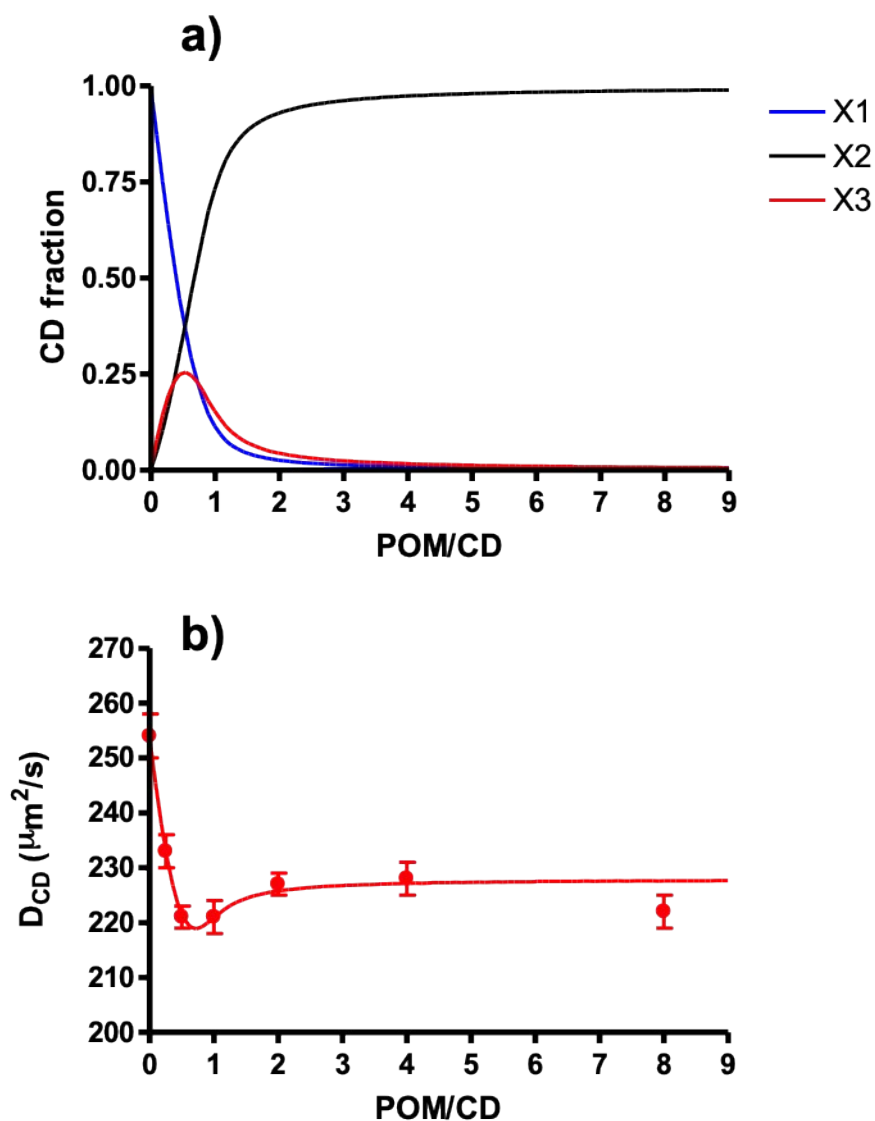


**Figure S19.** (a)  $\gamma$ -CD species distribution in two-step process model ( $X_1$ : free CD,  $X_2$  &  $X_3$ : 1:1 & 1:2 POM-CD complexes) as a function of POM/CD molar ratio  $R$  in the NMR experimental conditions for titration of 2 mM  $\gamma$ -CD by  $[\text{SiW}_{12}\text{O}_{40}]^{4-}$ . (b) Modeling of observed diffusion coefficient of  $\gamma$ -CD as a function of POM/CD molar ratio during titration of 2 mM  $\gamma$ -CD by  $[\text{SiW}_{12}\text{O}_{40}]^{4-}$ . The lines represent calculated curves with using equations 8-11  $K_{11} = 17000 \text{ M}^{-1}$ ,  $K_{12} = 460 \text{ M}^{-1}$  and diffusion coefficients limits for free CD, 1:1 and 1:2 complexes:  $D_1 = 254 \mu\text{m}^2/\text{s}$ ,  $D_2 = 226 \mu\text{m}^2/\text{s}$ , and  $D_3 = 163 \mu\text{m}^2/\text{s}$ .



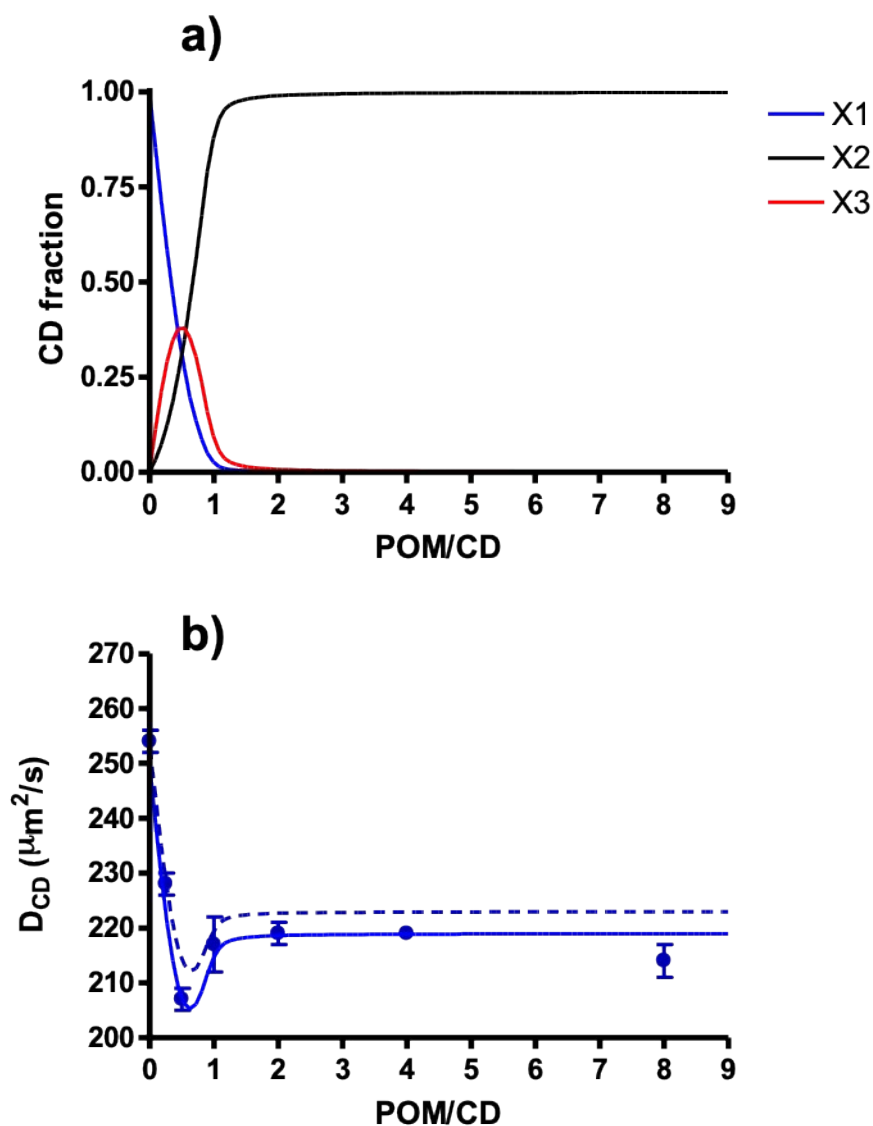


**Figure S20.** (a)  $\gamma$ -CD species distribution in two-step process model ( $X_1$ : free CD,  $X_2$  &  $X_3$ : 1:1 & 1:2 POM-CD complexes) as a function of POM/CD molar ratio  $R$  in the NMR experimental conditions for titration of 2 mM  $\gamma$ -CD by  $[\text{PW}_{12}\text{O}_{40}]^{3-}$ . (b) Modeling of observed diffusion coefficient of  $\gamma$ -CD as a function of POM/CD molar ratio during titration of 2 mM  $\gamma$ -CD by  $[\text{PW}_{12}\text{O}_{40}]^{3-}$ . The lines represent calculated curves with using equations 8-11  $K_{11} = 160000 \text{ M}^{-1}$ ,  $K_{12} = 1500 \text{ M}^{-1}$  and diffusion coefficients limits for free CD, 1:1 and 1:2 complexes:  $D_1 = 254 \mu\text{m}^2/\text{s}$ ,  $D_2 = 219 \mu\text{m}^2/\text{s}$  (full line) or  $D_2 = 226 \mu\text{m}^2/\text{s}$  (dashed line), and  $D_3 = 163 \mu\text{m}^2/\text{s}$ . The dashed line represents the expected behavior consistent with results obtained with previous POMs. The difference may indicate contribution from presence of other  $\text{PW}_{12}$ -CD species than 1:1 and 1:2 adducts suggesting a much more complex system and a two-step complexation process alone may be not enough for a full description of all phenomena taking place in solution.

## Part 5: SAXS measurements

### 1- Experimental

Small Angle X-ray Scattering (SAXS) measurements using Mo radiation ( $\lambda = 0.071$  nm) were performed on a bench built by XENOCS. The scattered beam was recorded using a large online scanner detector (diameter: 345 mm, from MAR Research). A large  $q$ -range ( $0.2$  to  $40$  nm<sup>-1</sup>) was covered with an off-center detection. The collimation was applied using a  $12:\infty$  multilayer Xenocs mirror (for Mo radiation) coupled to two sets of scatterless FORVIS slits providing a  $0.8 \times 0.8$  mm X-ray beam at the sample position. Pre-analysis of the data was performed using FIT2D software. The scattered intensities are expressed versus the magnitude of scattering vector  $q = [(4\pi)/\lambda]\sin(\theta/2)$ , where  $\lambda$  is the wavelength of incident radiation and  $\theta$  the scattering angle. 2 mm quartz capillaries were used as sample containers for the solutions. Usual corrections for background (empty cell and detector noise) and intensity normalization using a high density polyethylene as a standard were applied. Experimental resolution was  $\Delta q/q = 0.05$ . Silver behenate in a sealed capillary was used as the scattering vector calibration standard. The concentrations of nonionic surfactant and POM were chosen to get a reasonable signal from the laboratory SAXS camera.

### 2- SAXS spectra of Keggin POMs in water

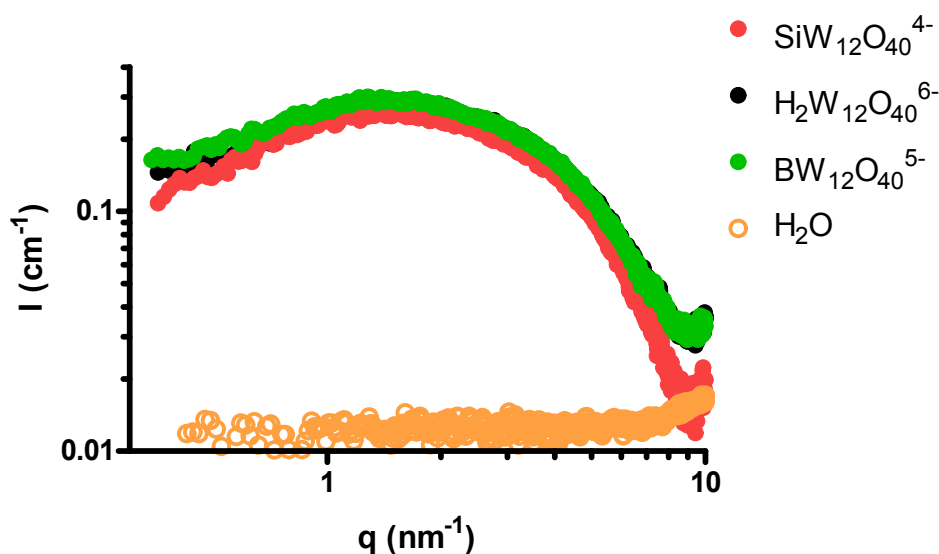


**Figure S21.** SAXS-spectra of 10 mM Keggin-POM in water for SiW<sub>12</sub>O<sub>40</sub><sup>4-</sup>, BW<sub>12</sub>O<sub>40</sub><sup>5-</sup> and H<sub>2</sub>W<sub>12</sub>O<sub>40</sub><sup>6-</sup>. The background scattering of water is additionally shown.

### 3- SAXS spectra of Keggin POMs in presence of $C_8E_4$

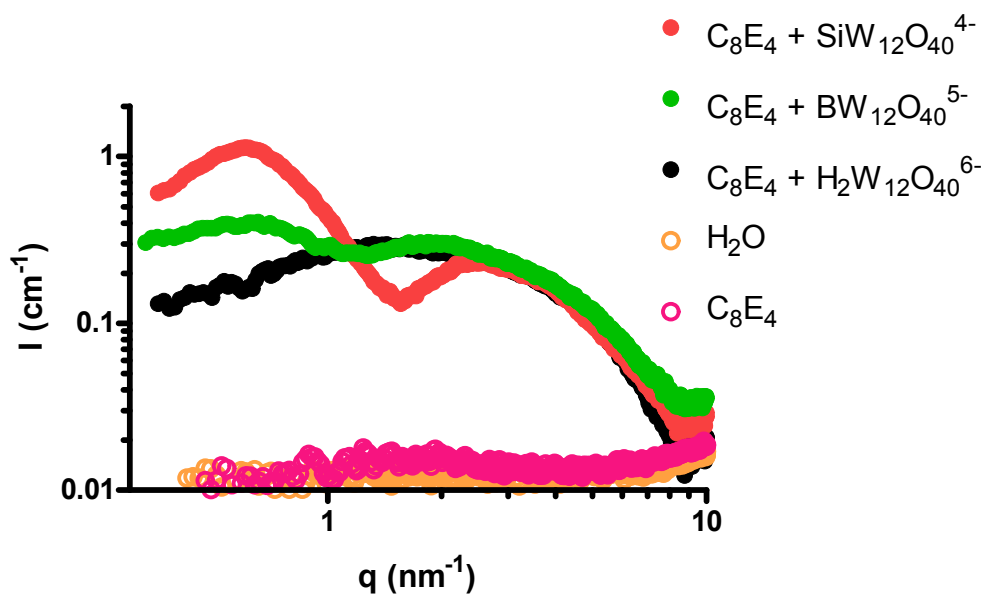


**Figure S22.** SAXS-spectra of 10 mM Keggin-POM + 60 mM  $C_8E_4$  in water for  $SiW_{12}O_{40}^{4-}$ ,  $BW_{12}O_{40}^{5-}$  and  $H_2W_{12}O_{40}^{6-}$ . The weak signal of 60 mM  $C_8E_4$  in the absence of POMs and the background scattering of water is additionally shown.

## Part 6: Characterizations by FT-IR spectroscopy

### 1- FT-IR spectrum of compound $\text{BW}_{12}\cdot 2\text{CD}$

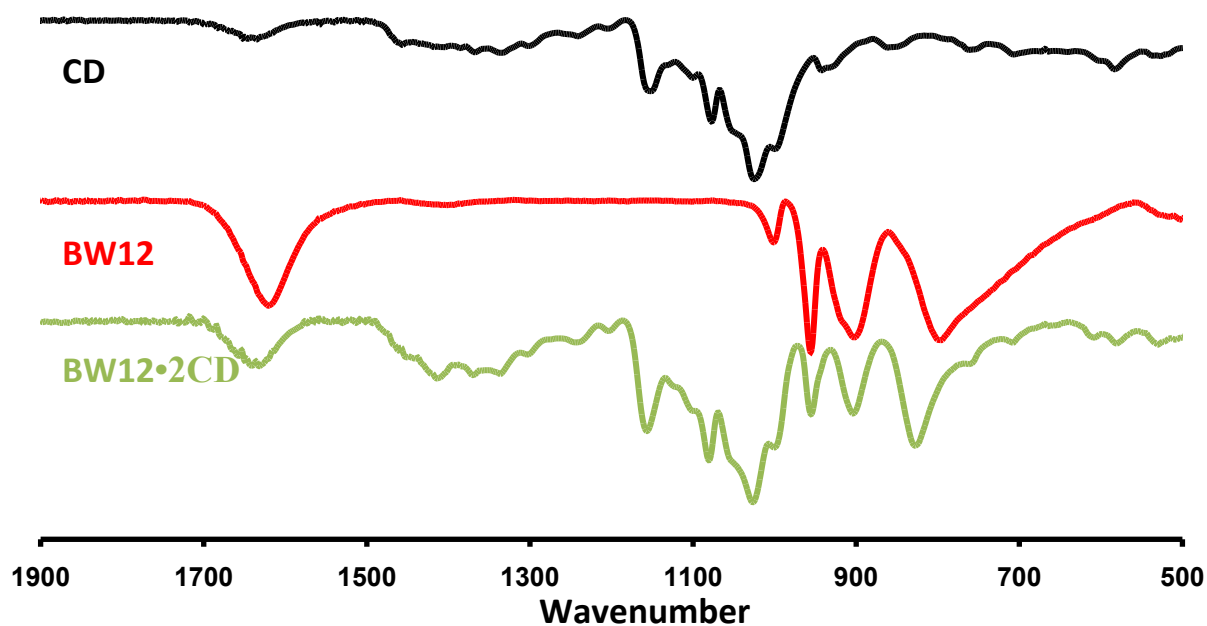


**Figure S23:** Infrared spectrum of  $\text{BW}_{12}\cdot 2\text{CD}$  in comparison with those of  $\text{K}_{4.3}\text{Na}_{0.7}[\text{BW}_{12}\text{O}_{40}]$ , and  $\gamma\text{-CD}$ . Absorption bands for  $\gamma\text{-CD}$  are observed at 1151 (1147) and 1022 (1018)  $\text{cm}^{-1}$ , and those for the POM appear at 995 (997), 953 (943), 899 (897), and 822 (806)  $\text{cm}^{-1}$ . The values in parentheses correspond to reference compounds.

## 2- FT-IR spectrum of compound $\text{PW}_{12}@CD$

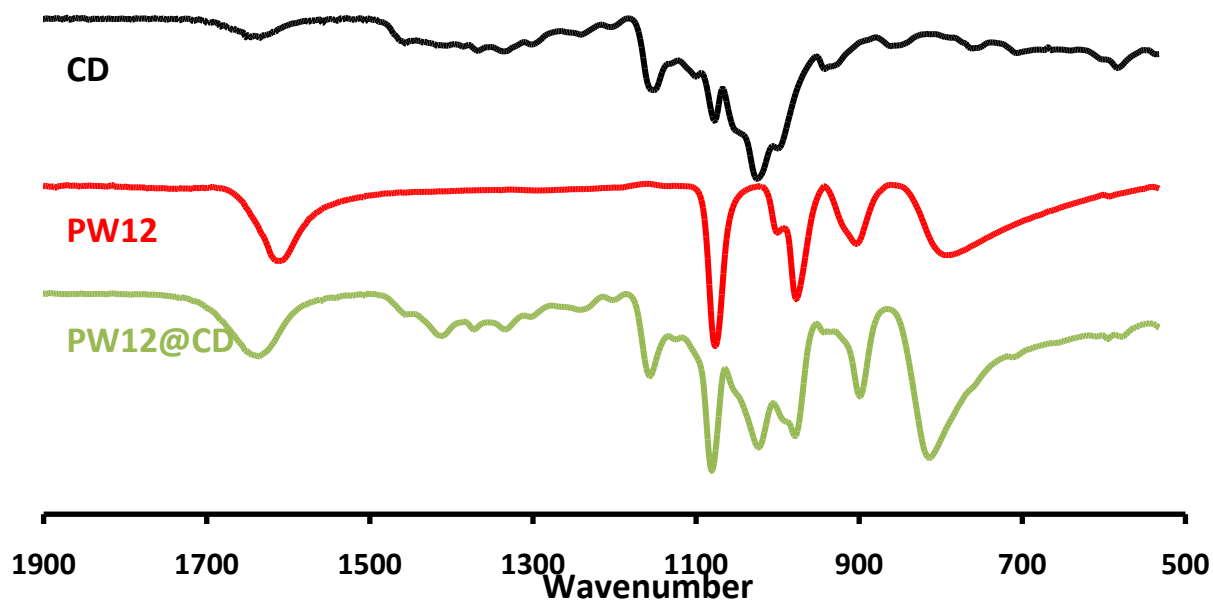


**Figure S24:** Infrared spectrum of  $\text{PW}_{12}@CD$  in comparison with those of  $\text{Na}_{1.4}\text{H}_{1.6}[\text{PW}_{12}\text{O}_{40}]$ , and  $\gamma\text{-CD}$ . Absorption bands for  $\gamma\text{-CD}$  are observed at 1151 (1147) and 1018 (1018)  $\text{cm}^{-1}$ , and those for the POM appear at 1078 (1074), 976 (974), 895 (899), and 806 (779)  $\text{cm}^{-1}$ . The values in parentheses correspond to reference compounds.